JOURNAL OF MATERIALS SCIENCE 18 (1983) 3143–3153

Mechanical properties of Sn–Ag_3Sn alloys

J. F. BROMLEY*, F. VNUK*, R. W. SMITH
Department of Metallurgical Engineering, Queen's University at Kingston, Ontario, Canada

The structure and properties of Sn–Ag_3Sn directionally-frozen eutectic alloys have been examined over the growth range 2×10^{-4} to 2×10^{-1} mm sec^{-1}. The structure is predominantly broken lamellar to 1.3×10^{-2} mm sec^{-1}, but with relatively poor alignment to the growth direction at smaller growth rates. The tensile and compressive strengths were measured. These increase monotonically to the growth rate at which cellular growth ensues, after which point they fall. The hardness of the eutectic closely parallels the compressive properties as the growth rate increases. Quenching from 200° C produces a marked increase in compressive strength and hardness, attributed to the quench-hardening of the Sn-rich phase.

1. Introduction

This work forms part of a long-term study of eutectic alloys undertaken to obtain a better understanding of how eutectics freeze and, therefore, how it might be possible to manipulate microstructure to obtain desirable mechanical and other physical properties in particular eutectics. Earlier studies have been concerned primarily with the development of a predictive morphological classification scheme [1–3]. As part of this work, it was shown that the so-called "anomalous" eutectics do exhibit a predictable freezing pattern, albeit somewhat more complex than that of simple regular lamellar (Al–$CuAl_2$) and rod-like (Sn–Cd) eutectics. Both phases in these simple eutectics grow in a non-faceted manner [1], whereas at least one phase in the anomalous eutectics is subject to faceting when freezing. It was found that the latter could be placed in four well defined categories by volume fraction (V_F), namely broken-lamellar, irregular, complex-regular and quasi-regular, with increasing volume fraction. We are now examining the extent to which the mechanical properties of each morphological group can be clearly characterized.

Since it is well known that the mechanical properties of an alloy are markedly structure sensitive, we are examining systematically a number of members of each group in an attempt to distinguish the contribution of phase morphology to the strength of a particular eutectic composite. To date we have reported work on Al–Si [4], Pb–Sb [5], Zn–Ge [6], Cd–Zn [7], Pb–Cd [8], Sb–Ge [9], Cd–Ge [10] and Sn–Zn [11].

This paper reports work on another member of the broken lamellar group of which we have already examined Cd–Ge ($V_F = 2.0\%$) and Sn–Zn ($V_F = 8.3\%$). It was found in these alloys that the mechanical properties did not obey the "rule of mixtures" prediction [12] and that large matrix constraints arose, even when the volume fraction of the faceting phase was only 2%. The Sn–Ag_3Sn eutectic ($V_F = 3.6\%$) was selected to further explore the extent to which such constraints are characteristic of the broken-lamellar microstructure group.

The Sn–Ag_3Sn eutectic contains 3.5% Ag and consists of an almost pure tin matrix (< 0.01% Ag), a body centred tetragonal structure with lattice parameters $a = b = 0.583$ nm and $c = 0.318$ nm [13], containing 3.6 vol% of the intermediate orthorhombic phase Ag_3Sn for which $a = 0.297$ nm, $b = 0.517$ nm and $c = 0.477$ nm [14]. This phase is almost stoichiometric, occurring from 73.2 to 74.5% Ag. Not surprisingly, the phase facets. The entropy of solution at the eutectic temperature is not known. Primaries of Ag_3Sn have been described as acicular as has the eutectic [15]. A better des-

* Present address: School of Metallurgy, SA Institute of Technology, Adelaide, SA 5000, Australia.

0022–2461/83 $03.00 + .12

cription for the eutectic phase would be ribbon-like but, as is commonly found with this structural group, the ribbons give way to fibres at higher growth rates [16]. Thus it is seen that the two eutectic phases are very different in crystal structure, and, with a volume fraction of only 3.6%, then neighbouring regions of the minor phase will be well separated. As a result, it was presumed that the mechanical properties might more closely follow the "rule of mixtures" prediction with virtually no matrix constraints such that the UTS (ultimate tensile strength) of the composite is the weighted mean of the bulk properties of the two phases.

2. Experimental details

Approximately 150 g samples of 99.999% purity components were melted in vacuum in sealed 7 mm i.d. Vycor tubes, shaken vigorously and then allowed to cool in the horizontal position to avoid macrosegregation. Unidirectional solidification was accomplished by lowering the specimen vertically through a tube-furnace in to a water bath at speeds from 2×10^{-4} to 1×10^{-1} mm sec^{-1} to produce a specimen 150 to 200 mm in length. The temperature gradient in the liquid (G_L) and in the solid (G_s) were measured by inserting thermocouples in the specimen tubes. It was found that $G_L \simeq 5^\circ$ C mm^{-1} and $G_s \simeq 3^\circ$ C mm^{-1} at $R = 1 \times 10^{-2}$ mm sec^{-1} and increased slightly as the growth rates fell. Also the rate of growth remained virtually constant during the freezing of any specimen.

After solidification, the specimens were removed from the Vycor tubes, and the leading 25 mm and trailing 20 mm were removed to ensure a completely eutectic specimen. Tensile specimens were nominally of gauge length 25.4 mm whilst compression specimens had a length to diameter ratio of 1.5. The latter were carefully ground to have flat parallel end faces. To avoid "barrelling", the ends of the compression specimens were lubricated with teflon tape coated with silicone grease.

Mechanical testing was performed on an Instron machine with a crosshead speed of 1 cm min^{-1} to give a strain rate, in tension, of $\simeq 7 \times 10^{-3}$ sec^{-1} and, in compression, of $\simeq 2 \times 10^{-2}$ sec^{-1}. The microhardness of the specimen also was measured.

Metallography proved somewhat difficult due to polishing-induced recrystallization artifacts. As a result, after diamond polishing, electropolishing was used in the standard perchloric acid bath. This also permitted the dissolution of the tin matrix. Etching, where necessary, was done with 10% Nital.

To achieve more rapid solidification than that possible with the apparatus referred to above, a "direct-chill" ingot mould was used [17]. This was approximately 25 mm diameter and was constructed to ensure unidirectional heat flow from the copper-chill base. Thus the rate of freezing of the alloy was a parabolic function of the distance of the solid/liquid interface from the base of the mould. This apparatus permitted the continuous correlation of structure with freezing rate. However, since some solid/liquid features require some finite time to develop, the direct chill specimens were used to interpolate between data from the fixed growth rate experiments described above.

3. Results

3.1. Microstructure

3.1.1. Ingots

If the eutectic alloys is furnace cooled, the microstructure shown in Fig. 1 is obtained. It is seen that the grain boundaries are very irregular suggesting the non-isothermal growth front reported for the Al–Si eutectic [18]. In contrast, more rapid cooling produces a modified eutectic structure and tin-rich primaries, Fig. 2. Further similarity to the behaviour of Al–Si alloys is seen in Fig. 3 in which a hypoeutectic alloy has been air cooled. Tin dendrites first appear and provide nucleation centres for the subsequent growth of the Sn–Ag_3Sn eutectic. Then, in Fig. 4, in the microstructure of the hypereutectic Sn–10% Ag alloy, air cooling caused coarse faceted Ag_3Sn primaries to be nucle-

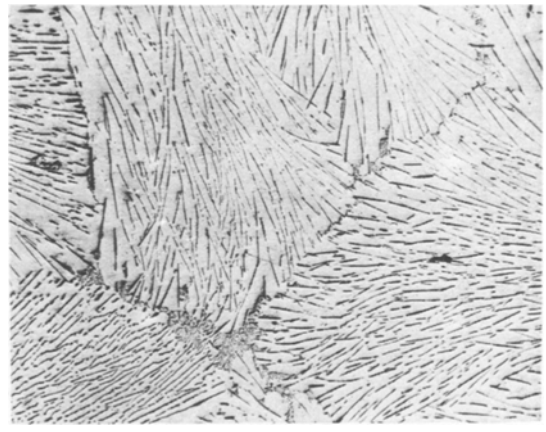

Figure 1 Furnace-cooled, eutectic Sn–Ag_3Sn (× 200).

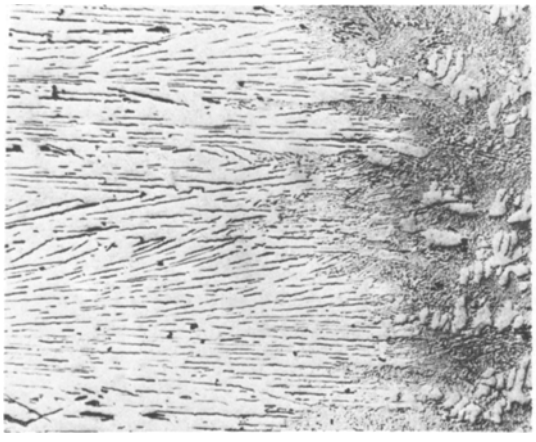

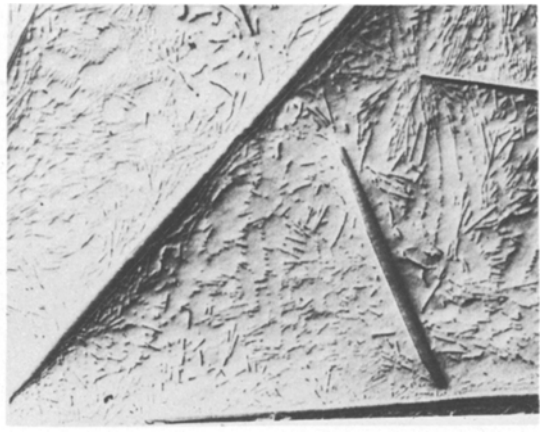

Ag_3Sn, directionally solidified, $R = 3.9 \times 10^{-2}$ mm sec^{-1} (× 300).

ated first but these were not effective nucleants for the tin phase. As a result the eutectic undercooled, the tin phase nucleated from the undercooled melt as a halo around the Ag_3Sn primaries, grew dendritically and then led to the production of a modified eutectic. This demonstrates clearly the non-reciprocal nucleation behaviour in this system.

3.1.2. Directionally solidified eutectic alloys

The microstructure of the directionally solidified eutectic was found to be growth-rate sensitive. When slowly frozen, the faceting Ag_3Sn phase consisted of flat plates or laths, with considerable misalignment in the transverse section (Fig. 5). In fact, the morphology of the Ag_3Sn phase may be quite variable in a single microscope section, often corrugated, Fig. 2.

As the growth rate was increased, the regularity of the ribbon increased and the interplate spacing decreased, Fig. 6. In some sections, the Ag_3Sn adopted a rod-like morphology, Fig. 7. Further increases in growth rate led to constitutional supercooling, cellular growth and the tell-tale colony structure, Fig. 8. Frequently, each cell was a columnar grain, Fig. 9.

In passing, it may be noted that the interparticle spacing in these eutectic alloys, and also that reported earlier [19] fitted the equation:

$$\lambda = 0.705R^{-0.50} \quad (1)$$

where λ is the interphase spacing (microns).

3.1.3. Directionally solidified off-eutectic alloys

Well aligned primaries and eutectic were observed in directionally frozen off-eutectic alloys. This was

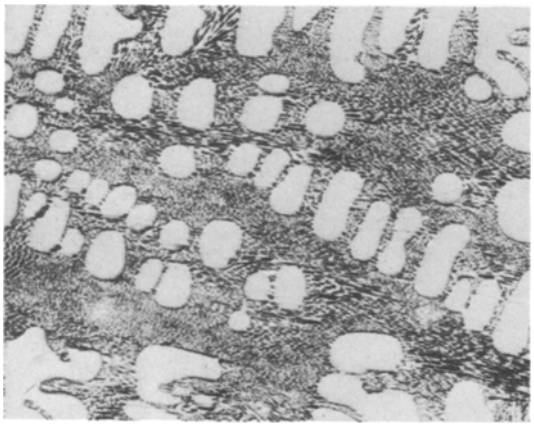

Figure 3 Air-cooled, hypoeutectic Sn–3.4% Ag (× 200).

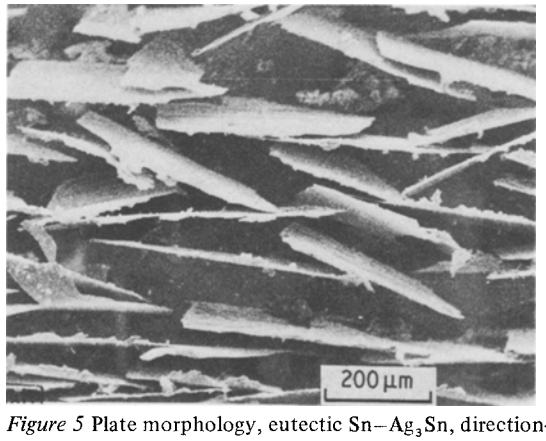

Figure 5 Plate morphology, eutectic Sn–Ag_3Sn, directionally frozen (SEM) transverse section $R = 2.2 \times 10^{-4}$ mm sec^{-1}.

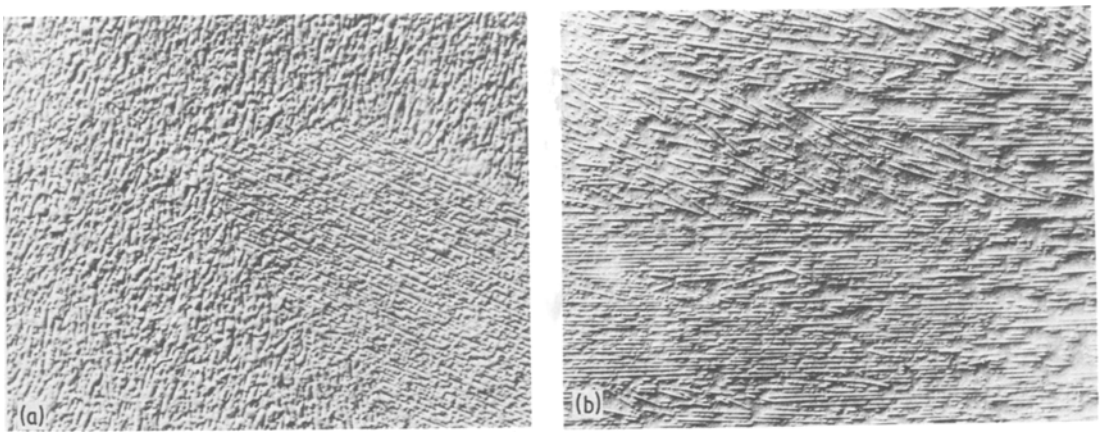

Figure 6 Plate morphology, eutectic Sn–Ag_3Sn, directionally frozen, $R = 1.3 \times 10^{-2}$ mm sec^{-1} (× 150). (a) Transverse Section; (b) Longitudinal Section.

particularly pronounced in the hypereutectic alloys, Fig. 10.

3.2. Mechanical properties

3.2.1. Tensile properties

Under normal conditions, tin and its alloys do not exhibit a yield point. Thus an 0.5% off-set proof stress was determined from the stress–strain curves shown in Fig. 11. The data is collected in Table I, where it is seen that the alloy displays a progressive increase in proof stress and ultimate tensile strength (UTS) with increasing growth speeds to a maximum at a solidification rate of 1.3×10^{-2}. As might be anticipated, this doubling in strength was accompanied with a halving of ductility. However, a further increase in speed produced a significant reduction in strength ($\simeq -20\%$) but a marked improvement of ductility ($\simeq +150\%$). The mechanical properties of the as-cast slow-cooled eutectic and pure tin in the annealed state are given for comparison.

Thompson *et al.* [20] have shown that in aligned eutectics, the lamellar spacing (λ) appears to play a role similar to that of grain size (d) in the interpretation of the mechanical properties of a polycrystalline specimen and so a Petch–Hall [21, 22] relationship of the form:

$$\sigma_y = \sigma_b + K_y \lambda^{-1/2} \qquad (2)$$

may be observed, where σ_y, σ_b and K_y are the

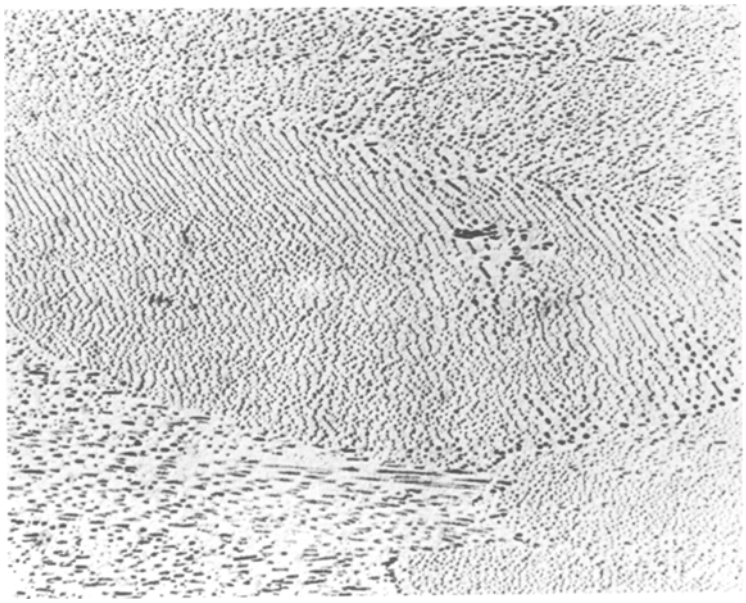

Figure 7 Rod-like morphology, eutectic Sn–Ag_3Sn directionally frozen $R = 3.9 \times 10^{-2}$ mm sec^{-1}, transverse section (× 100).

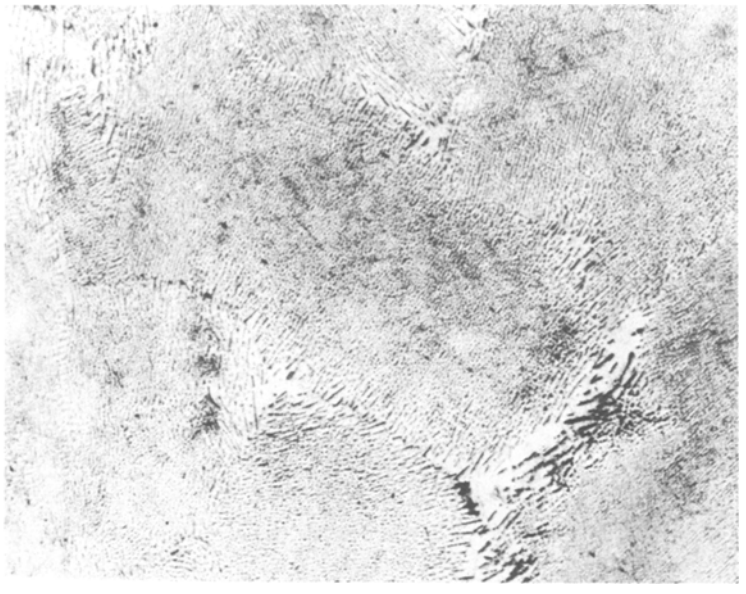

Figure 8 Cellular growth, eutectic $Sn-Ag_3Sn$ directionally frozen, $R = 1.2 \times 10^{-1}$ mm sec^{-1}, transverse section (×100).

yield stress, friction stress and a constant, respectively. In addition, since λ is inversely proportional to the square root of the freezing rate (R) [23], then

$$\sigma_y = \sigma_b + K'R^{1/4} \quad (3)$$

A more general form of this expression has been observed to adequately describe the effects of growth rate [7], namely:

$$\sigma = \sigma_0 + K'R^n \quad (4)$$

where n has been shown to vary between 0.25 and 0.50.

If the strength parameters are plotted on a log/log plot, Petch–Hall type expressions (Equation 3) may be fitted to them by a regression analysis (Fig. 12). Thus for $R < 2 \times 10^{-3}$ mm sec^{-1}:

$$\lambda_y = 10.1 + 889R^{0.46} \quad (5)$$

where λ_y is the 0.5% offset proof stress in N mm^{-2}. Similarly

$$\lambda_u = 19.2 + 372R^{0.35} \quad (6)$$

when λ_u is the UTS in N mm^{-2}.

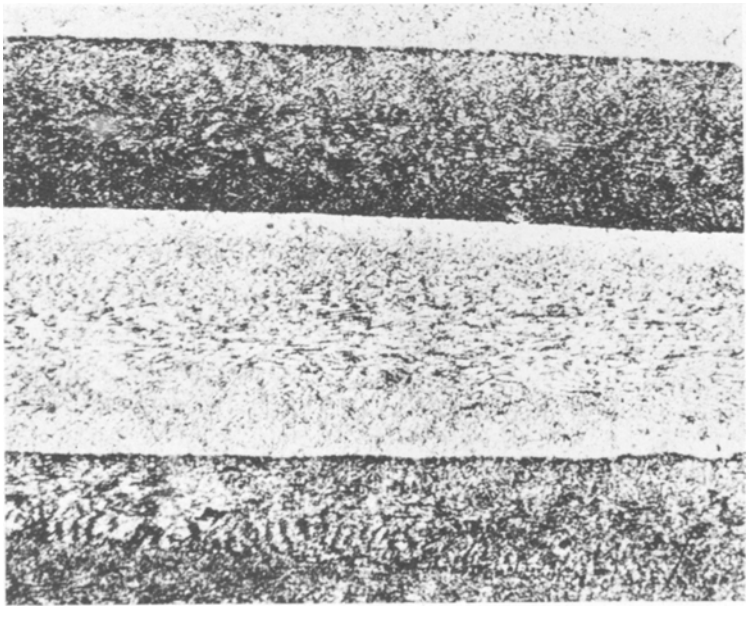

Figure 9 Cellular growth, eutectic $Sn-Ag_3Sn$, directionally frozen, $R = 1.2 \times 10^{-1}$ mm sec^{-1}, longitudinal section.

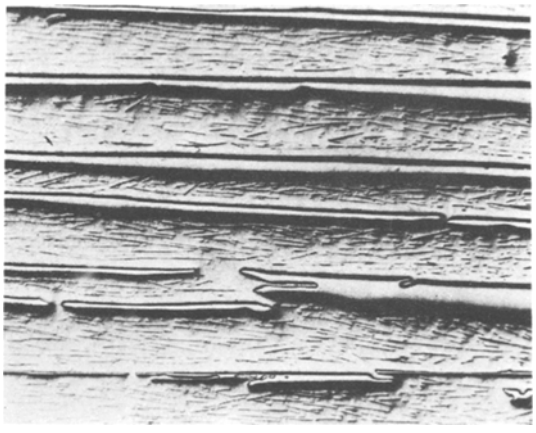

Figure 10 Directionally-frozen, hypereutectic alloy, $R = 1.3 \times 10^{-2}$ mm sec^{-1} (× 100).

3.2.2. Compressive properties

Values of the 0.5% off-set compressive proof stress (λ_c) are shown also in Table I and Fig. 12. As with the tensile strength values, a Petch–Hall expression may be fitted to them for $R < 1.3 \times 10^{-2}$ mm sec^{-1}

$$\lambda_c = 33.8 - 209R^{0.29} \quad (7)$$

where λ_c is in N mm^{-2}.

3.2.3. Effect of heat-treatment on mechanical properties

Elsewhere [24], we have shown that when the tin-rich phase of this eutectic is quenched from near the eutectic temperature, a marked increase in hardness results. In view of this, samples grown at the various speeds described earlier were held at 200° C for 1/2 h and then water-quenched. A significant increase in compressive strength was obtained, Fig. 13. The heat-treated specimen data was found to be described by:

$$\lambda_H = 43 + 225R^{0.28} \quad (8)$$

where λ_H is the 0.5% offset compressive proof stress in N mm^{-2}, valid to $R = 1.3 \times 10^{-2}$ mm sec^{-1}. Also in Fig. 13 are the Vickers Hardness values for the as-grown specimens. After heat-treatment, all specimens displayed the same hardness value, namely 18.5 kg mm^{-2}, which compares closely with the value of saturated Sn–Ag alloys quenched from 200° C. This value is above the maximum value obtained from specimens strengthened by Ag_3Sn second phase reinforcement alone.

4. Discussion

4.1. Microstructure

It is interesting to compare the microstructures of the unidirectionally grown Sn–Ag_3Sn eutectic ($V_F = 3.5\%$) with the two other members of the broken lamellar structure group, namely, Sn–Zn ($V_F = 8.3\%$) [11] and Cd–Ge ($V_F = 2.0\%$) [10]. The lamellae in the Sn–Zn eutectic at $R \simeq 10$ mm h^{-1} are perforated but very regular, permitting the interlamellar spacing to be measured precisely at 2 μm. However, the Cd–Ge eutectic displays much less regularity and was observed to have the large, well-developed and aligned lamellae spaced some 35 μm apart, with finer arrays of the faceting phase dispersed between them.

The Sn–Ag_3Sn, with a V_F value closer to that of the Cd–Ge eutectic, tends to display an intermediate microstructural pattern but with significantly less interlamellar debris, Fig. 6. The corresponding interlamellar spacing is 6 μm.

The Sn–Ag_3Sn eutectic structure becomes modified at higher growth rates ($R \geqslant 2 \times 10^{-2}$ mm h^{-1}) to give a fibrous eutectic and tin-rich pri-

TABLE I Summary of tensile and compressible test results

	Growth speed (mm sec^{-1})	0.5% off-set tensile proof stress (N mm^{-2})	Ultimate strength (N mm^{-2})	Per cent elongation (%)	Per cent reduction in area (%)	0.5% off-set compressive proof stress (N mm^{-2})
1.	2.2×10^{-4}	29.0	39.0	45	57	51.5
2.	6.6×10^{-4}	42.5	50.0	27	55	60.2
3.	2.0×10^{-3}	61.5	64.5	22	50	73.6
4.	1.3×10^{-2}	62.1	65.3	22	82	90.7
5.	3.9×10^{-2}	54.1	55.0	40	90	77.6
6.	1.2×10^{-1}	42.3	51.7	55	91	71.8
Slowly cooled as-cast		15.0	36.6	39	72	44.3
Pure annealed tin		7.35	12.4	120	100	13.3

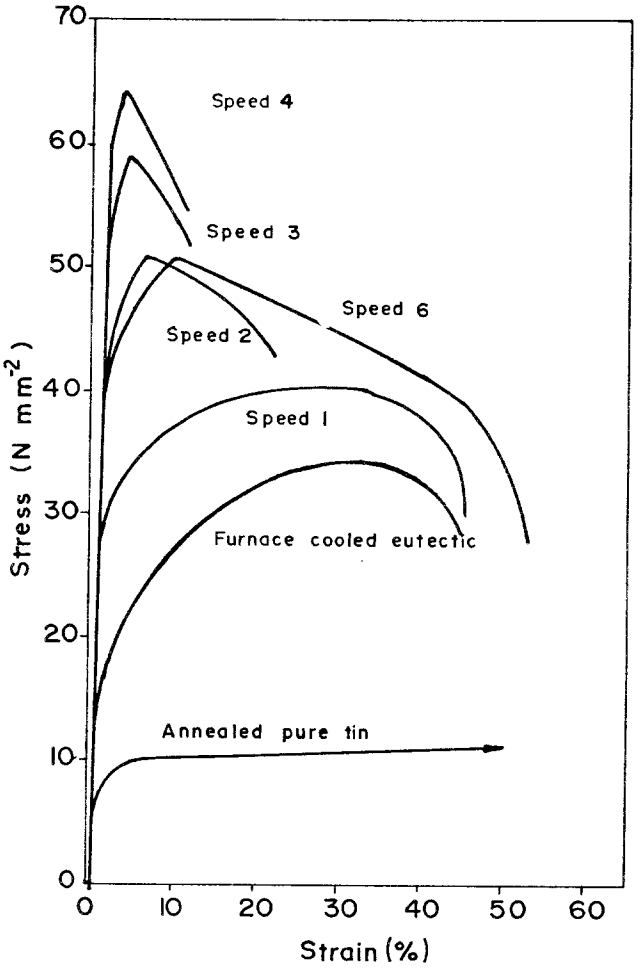

Figure 11 Stress–strain curve, eutectic Sn–Ag_3Sn, directionally frozen at speeds given in Table I.

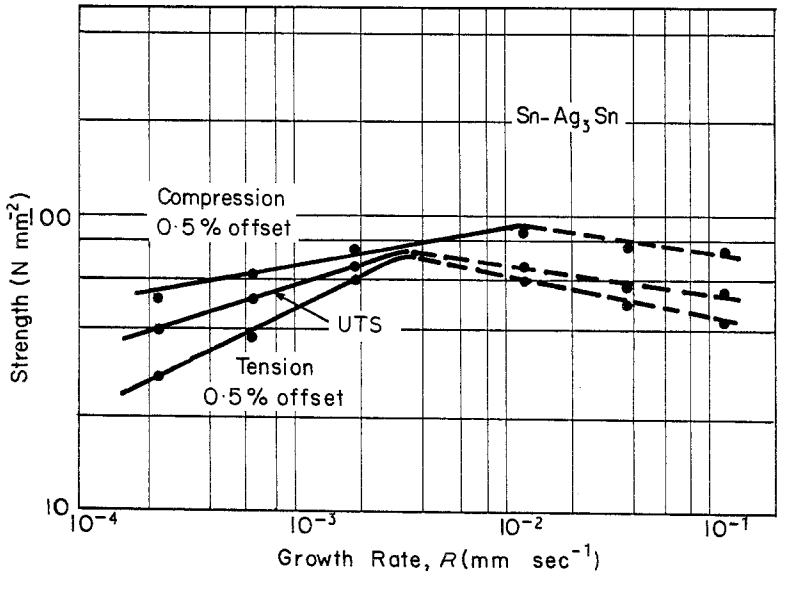

Figure 12 Strength parameter against growth rate, eutectic Sn–Ag_3Sn, directionally frozen.

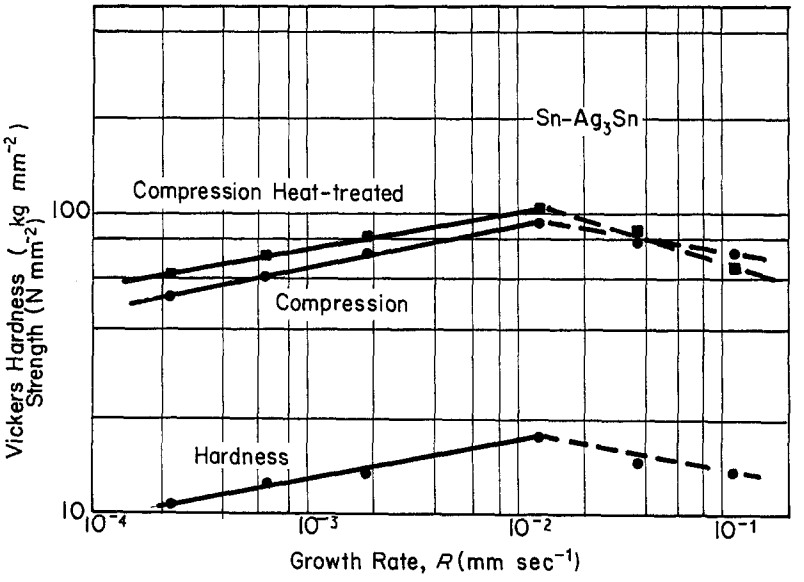

Figure 13 Variation in compressive 0.2 off-set proof stress and hardness against growth rate, eutectic $Sn-Ag_3Sn$, directionally frozen.

maries. This behaviour closely parallels that of Cd–Ge but is in marked contrast to that of Sn–Zn eutectic alloys where no primaries were observed even at growth rates of 4000 mm h^{-1}.

It was noted that, at times, the Ag_3Sn phase adopted a corrugated ribbon morphology. Similar behaviour has been reported for silicon in Al–Si eutectic alloys [25]. In the latter case, it was shown that corrugations would form during growth with small temperature gradients in the liquid. Such were used in this study, but Southin and Jones [26], using large temperature gradients, did not observed corrugated growth in the Ag_3Sn phase. In the past, such "wavy" growth has been seen in other regular lamellar eutectics at very small freezing rates and has been associated

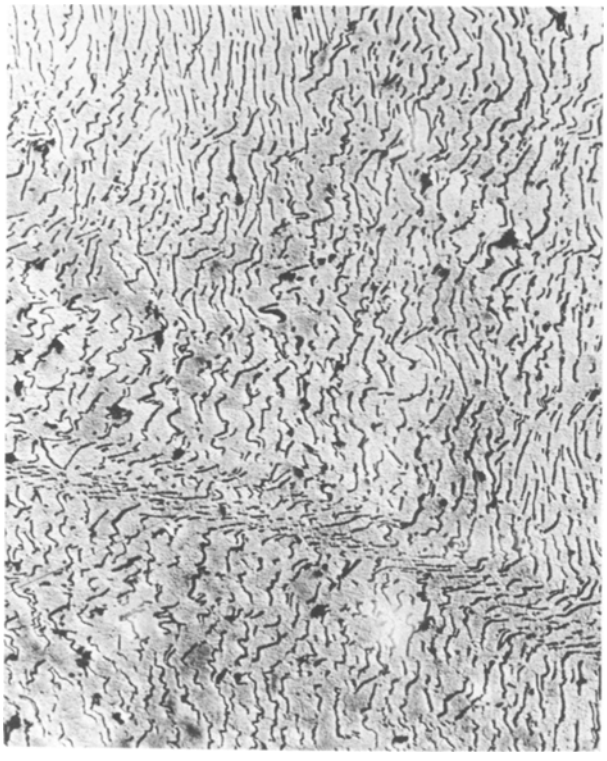

Figure 14 Eutectic $Sn-Ag_3Sn$, directionally solidified and compressed, longitudinal section (× 200).

with the crystallographic rotation of the phases [27].

4.2. Mechanical properties

It is instructive to calculate a "reasonable" value for the Sn–Ag_3Sn eutectic composite following the rule of mixtures. In order to do this it is necessary to know the mechanical properties of the two phases and the geometrical arrangement of the phases in order to modify the simple theory developed for continuous regular filaments [28, 29]. Usually such information is not available, since, even if the fibres are extracted and their mechanical properties determined, the fibres, *in situ*, may deform in a different manner [28]. For example, when the Sn–Ag_3Sn eutectic composite is compressed, the normally brittle Ag_3Sn phase is seen to undergo considerable plastic deformation, Fig. 14. Also, the differing coefficients of thermal expansion between reinforcing phase and matrix can influence behaviour. Commonly, the matrix is left in tension and the reinforcing phase in compression when the composite has cooled to room temperature. As a result, for systems with a small V_F value the composite yields at a lower stress in tension than in compression. This behaviour was observed in the Cd–Ge eutectic [10] and may be observed here. However, this reduced strength may also arise from local premature brittle failure of the Ag_3Sn phase. In view of this sort of unresolved qualification, the composite strength predicted by the rule of mixtures may be only an approximation and so the application of more rigorous derivations of the law of mixtures is not justified.

An approximate value for the strength of the Sn–Ag_3Sn composite may be obtained as follows. The UTS of melt-spun filaments of Ag_3Sn has been reported as 340 MN mm^{-2} [29]. The measured UTS of the as-cast zone-refined tin used to make the eutectic was found to be 12.5 MN mm^{-2}, whereas the value reported for (commercially) "pure" tin is 14.5 MN mm^{-2} [15]. In view of the fact that the Sn-rich phase in the eutectic contains some silver as solute, then some solid-solution strengthening is likely and so the higher value is considered to be more suitable for use in any calculation.

Since the Ag_3Sn phase is not present as continuous regular fibres, it is necessary to calculate whether its aspect ratio exceeds the critical value. This is given by [30]:

$$\frac{l_c}{d_f} = \frac{\sigma_{f\,max}}{2T} \tag{9}$$

where l_c is the critical fibre length (mm), d_f is the fibre diameter (mm), $\sigma_{f\,max}$ is the average maximum fibre strength (N mm^{-2}), T is the ultimate shear strength of the matrix (N mm^{-2}). The value of the ultimate shear strength may be related to an interfacial shear stress which, in a perfectly bonded yielding matrix, may be approximated to half the uniaxial tensile yield stress [31]. Thus, Equation 9 reduces to:

$$\frac{l_c}{d_f} = \frac{\sigma_{fm}}{\sigma_{m\mu}}. \tag{10}$$

Substituting $\sigma_{fm} = 340$ MN mm^{-2} and $\sigma_{m\mu} = 14.5$ MN mm^{-2} in Fig. 10 results in a critical aspect ratio $(l_c/d_f) = 26$. Observation of the microstructure (Fig. 6) suggests that this value is easily achieved. This was confirmed by an examination of the fracture surfaces of tensile specimens, all of which showed no "pull-out" of fibres.

In addition to the requirement that the reinforcing phase possess an aspect ratio exceeding a critical value, it must also exceed a critical volume fraction [7, 32]. In normal circumstances, this may be approximated by:

$$V_{crit.} = \frac{\sigma_{m\mu} - \sigma_m}{\sigma_{fm} - \sigma_m} \tag{11}$$

when σ_m = yield strength of the matrix. For pure tin $\sigma_m \simeq 7.5$ N mm^{-2} and so, substituting appropriate values in Equation 11, it is found that $V_{crit.} = 1.9\%$. Since the Sn–Ag_3Sn eutectic contains 3.6% of the strengthening Ag_3Sn phase, this system should qualify as a fibre-strengthened composite.

The strength of this composite may be calculated [31] since:

$$\sigma_c = \sigma_f V_f + \sigma_m(1 - V_f). \tag{12}$$

Thus, σ_c is 21 or 28 MPa depending on whether the yield stress or the UTS is used as the value for σ_m. However, it should be noted that this would be an upper value since no account has been taken of the extent to which fibre discontinuities and poor alignment would serve to decrease the expected strength.

Comparing the value of 28 MPa with the lowest σ_c value in Table I, namely 39 MPa at a growth rate of 2.2×10^{-4} mm sec^{-1}, it is seen that the theoretical value is somewhat lower than the experimental values. In view of this, it is seen that

matrix constraints are present even with only $V_F = 3.6\%$.

The strength of a composite is not only related to the gross fibre concentration, but also to the fibre distribution. Since the fibre alignment and spacing was seen to become more uniform as the freezing rate was increased, the observed increase in strength might well be expected. So, too, should be the sharp decrease associated with the onset of cellular growth since here the regularity and uniformity of the Ag_3Sn spacing is changed markedly.

As noted earlier, the mechanical properties of the eutectic as a function of Ag_3Sn spacing, and therefore growth rate, may be described by a modified Petch–Hall expression (Equation 4). This permits the specification of a growth-rate independent portion of the strength, σ_0, which characterizes the composite in terms of the volume fraction, type and the morphology of the reinforcing phase present. The second term expresses the growth rate dependence of the second phase spacing. Usually, it is only possible to do this over a limited freezing range where the structural type is well defined, i.e. below the growth rate where, for example, cellular growth takes place or where some other marked structural transition takes place.

For the Sn–Ag_3Sn eutectic, it is seen that the exponent of the growth-rate dependent term for the 0.5% off-set proof stress is 0.46 in tension and 0.29 in compression. It was noted that, during testing, whilst the tensile deformation was primarily by slip, audible clicking accompanied compressive deformation, indicating twinning, (Fig. 14). The accepted value of E (Young's modulus) for tin is 4.14×10^4 MPa [15], whilst, for Ag_3Sn fibres, a value of 2.3×10^4 MPa [14] has been reported. The latter is of the same magnitude as that for polymers and graphite, whilst hard intermediate compounds tend to have values greater by a factor of ten. If this value for Ag_3Sn is correct (it came from four tensile tests), the tin matrix would be plastically deforming before the fibres could begin to support the matrix. This would produce premature misalignment, the buckling of fibres and, hence, premature failure.

By comparison, in the Cd–Zn eutectic [7] exponents of 0.25 and 0.20 were observed for slip and twin-controlled yielding, respectively. Similarly, for the Mg–Mg_2Ni eutectic composite [32], slip controlled yielding gave an exponent of 0.5 whilst twinning produced a value of 0.3. Thus it would appear that, commonly, the exponent for slip-controlled deformation is higher than that for twin-controlled deformation.

It is interesting to note the microhardness and compressive strength before and after heat treatment. It is seen that these closely parallel each other, e.g. the slopes of the graphs as determined by the measured exponents of the fitted curves are 0.29 and 0.26 for compressive strength and Vickers microhardness, respectively. Hence, the variation of these parameters with R show quite reasonable correlation. Correlation of hardness with tensile strength was poor, as the exponent of the UTS curves is 0.35. Similarly, a markedly better correlation of hardness with compressive strength was seen in Al–Si eutectic alloys [17].

5. Conclusions

1. Sn–Ag_3Sn eutectic alloys have been directionally solidified at rates from $2 \times 10^{-4} \rightarrow 2 \times 10^{-1}$ mm sec^{-1}. The structure was found to be markedly growth rate sensitive. At the lowest speed, the faceting Ag_3Sn phase consisted of flat plates or laths, with considerable misalignment displayed in transverse microsections. Interplate spacing decreased and alignment to the growth direction increased as the freezing rate increased.

2. A transition to rod-like growth was seen to have occurred in some grains at $R = 1.3 \times 10^{-2}$ mm sec^{-1}. Cellular growth occurred at higher growth rates, giving a colony structure.

3. Non-reciprocal nucleation of the eutectic phases was observed, the Ag_3Sn primaries possessing a Sn-rich halo.

4. Well-aligned unbranched Ag_3Sn primaries were produced in hypereutectic alloys.

5. Tensile and compressive strengths increased monotonically with growth rate to the point at which cellular growth took place, after which the strength fell. These data could be described by a Petch–Hall expression, the growth-rate dependent exponent of which appeared sensitive to the principal deformation mode during yielding, i.e. the exponent for slip-dominated deformation being higher than when twinning occurs.

6. The change of hardness with growth rate more closely resembled the change of compressive strength.

7. The actual strength of the eutectic composite was significantly higher than that predicted by the rule of mixtures.

8. Quenching the eutectic from 200° C pro-

duced a marked increase in compressive strength due to the quench hardening of the tin-rich phase.

Acknowledgements

The authors wish to acknowledge the financial support of the National Research Council of Canada and of Queen's University.

References

1. M. N. CROCKER, R. S. FIDLER and R. W. SMITH, *Proc. Roy. Soc.* **A335** (1973) 15.
2. M. N. CROCKER, M. McPARLAN, D. BARAGAR and R. W. SMITH, *J. Cryst. Growth* **29** (1975) 85.
3. M. N. CROCKER, D. BARAGAR and R. W. SMITH, *ibid.* **30** (1975) 198.
4. M. SAHOO and R. W. SMITH, *Met. Sci.* **9** (1975) 217.
5. *Idem, Can. Met. Quart.* **15** (1976) 1.
6. *Idem, J. Mater. Sci.* **11** (1976) 1125.
7. *Idem, ibid.* **11** (1976) 1680.
8. *Idem, ibid.* **13** (1978) 283.
9. *Idem, ibid.* **13** (1978) 1565.
10. M. SAHOO, G. W. DELAMORE and R. W. SMITH, *ibid.* **15** (1980) 1097.
11. F. VNUK, M. SAHOO, D. BARAGAR and R. W. SMITH, *J. Mater. Sci.* **15** (1980) 2573.
12. H. BIBRING, "Proceedings of the Conference on In-Situ Composites," Vol. II (National Academy of Engineering, Washington, DC, 1973) p. 1.
13. G. H. SISTARE, "Metallorgraphy, Structures and Phase Diagrams," ASM Metals Handbook, Vol. 8 (1973) p. 256.
14. J. V. WOOD and S. C. KING, *J. Mater. Sci.* **13** (1978) 1119.
15. C. J. THWAITES, "Microstructure of Tin and Tin Alloys," ASM Metals Handbook, Vol. 7 (1972), 317.
16. V. de L. DAVIES, *J. Inst. Met.* **93** (1964–65) 10.
17. F. VNUK, M. SAHOO, R. VAN de MERWE and R. W. SMITH, *J. Mater. Sci.* **14** (1979) 975.
18. M. R. DAY and A. MELLAWELL, *Proc. Roy. Soc.* **A305** (1968) 473.
19. A. MOORE and R. ELLIOTT, "The Solidification of Metals", Publ. 110. (Iron and Steel Institute, 1968) p. 213.
20. E. R. THOMPSON, F. D. GEORGE and E. M. PREINAN, Publ. NMAB–308–11 pp. 71–78, (National Academy of Science, Washington DC, 1973).
21. N. J. PETCH, *J. Iron Steel Inst.* **173** (1953) 25.
22. E. O. HALL, *Proc. Phys. Soc.* **64B** (1957) 747.
23. F. D. LEMKEY, R. W. HENTBERG and G. A. FORD, *Met. Trans. Soc. AIME* **233** (1965) 338.
24. F. VNUK, M. H. AINSLEY and R. W. SMITH, *J. Mater. Sci.* **16** (1981) 1171.
25. M. G. DAY, "The Solidification of Metals," Publ. No. 110 (Iron and Steel Institute, 1968) p. 177.
26. R. T. SOUTHIN and B. L. JONES, *J. Aust. Inst. Met.* **13** (19688) 203.
27. A. HELLAWELL, "The Solidifcation of Metals," Publ. No. 110 (Iron and Steel Institute, 1968) p. 177.
28. R. W. HERTZBERG, "Fibre Composite Materials" (ASM, 1964).
29. A. KELLY and W. R. TYSON, "Fibre Strengthened Materials," Second International Materials Symposium, University of California, (1964).
30. R. H. KROCKEL and J. BROUTMAN, "Modern Composite Materials" (Addison-Wesley Publishing Co., 1967).
31. D. W. PETRASEK, R. A. ISGNOVELLI and J. M. WEETON, "Fibre Strengthened Metallic Composites" (ASTM, 1967) p. 149.
32. K. H. ECKELMEYER and R. W. HERTZBERG, *Met. Trans.* **3** (1972) 609.

Received 25 January
and accepted 24 February 1983